Journal Code	Article ID	Dispatch: 03-OCT-18	CE: Bargavi
APP	47257	No. of Pages: 13	ME:

JOURNAL OF Applied Polymer SCIENCE

PHBV/TPU/cellulose compounds for compostable injection molded parts with improved thermal and mechanical performance

Estefanía Lidón Sánchez-Safont,[1] Alex Arrillaga,[2] Jon Anakabe,[2] ~~José~~ Gamez-Perez,[1] Luis Cabedo[1]

[1]Polymers and Advanced Materials Group (PIMA), Universitat Jaume I, Av. Vicent Sos Baynat s/n, 12071 Castelló, Spain

[2]Leartiker S. Coop., Xemein etorbidea 12, 48270 Markina-Xemein, Spain

Correspondence to: L. Cabedo (lcabedo@uji.es)

ABSTRACT: Poly(hydroxybutyrate-*co*-valerate) (PHBV) is a biopolymer that has gained a lot of attention because of its biodegradability, good thermal resistance, and balanced mechanical properties with respect to some commodity plastics. However, it presents two big limitations that hinder its potential application in replacing plastics for rigid injected parts: high cost and low toughness. Aiming at overcoming these limitations, the use of two additives in a PHBV matrix was explored: thermoplastic polyurethane (TPU) as an impact modifier and cellulose as reinforcing filler. Compounds of PHBV with different TPUs and cellulose contents were prepared by extrusion and, subsequently, injection molding. The morphology, thermal, and mechanical properties of the so-obtained materials were analyzed. Also, the biodisintegrability under standard composting conditions of the studied compositions was also assessed. The results of this work show that the obtained PHBV/TPU/cellulose compounds are biodisintegrable and show balanced properties in terms of thermal resistance–stiffness–toughness. These properties point these compounds as potential candidates to replace commodities in rigid part applications that require biodisintegration in their end-of-life, being able to be processed in a conventional injection molding industrial facility. © 2018 Wiley Periodicals, Inc. J. Appl. Polym. Sci. **2018**, *00*, 47257.

Received 28 May 2018; accepted 13 September 2018

DOI: 10.1002/app.47257

INTRODUCTION

One of the most extended applications of polymeric materials are the injection molded rigid parts, for a wide range of products in automotive industry, domestic appliance, toys, biomedical, packaging, and so forth. Commonly used materials for injected applications include polypropylene (PP) and polystyrene (PS), high impact PS, or acrylonitrile–butadiene styrene (ABS), and their use is widely extended because of their easily processing, low cost and overall mechanical properties (stiffness, tensile strength, and toughness), which makes them especially adequate for these type of applications. In addition, these materials usually have a high thermal resistance with heat deflection temperatures (HDTs) over 90 °C that allow their use in applications where relatively high temperatures are required.

Nowadays, there is an increasing interest in finding sustainable alternatives to these commodity polymers, in order to diminish the environmental impact associated to consumer products, and more specifically, the impact associated with their wastes. One of the most promising approaches driven to reduce the post-consumer plastics environmental impact is the use of biodegradable systems that enable their composting together with the organic fraction of the municipal wastes.[1] Polyhydroxyalkanoates (PHAs) are within the different biodegradable alternatives to rigid thermoplastics with a high HDT.[2] The PHAs are a family of bacterial polyesters that are biodegradable, biocompatible, and nontoxic.[3–5] In particular, poly(hydroxybutyrate-*co*-valerate) (PHBV), a thermoplastic copolyester from the PHAs family has gained a lot of attention because of its commercial availability, its physicochemical properties close to that of some of the commodities such as PP,[6] because it can be processed using conventional thermoplastic equipment and have equilibrate mechanical properties in terms of stiffness and tensile strength. However, PHBV presents two big limitations that restrict its use in these types of applications: high cost and low toughness (low impact resistance).[7,8]

With the aim of overcoming these two limitations, within an industrial approach, the addition of two different components to PHBV will be explored. In order to reduce the brittleness of PHBV, an elastomer as an impact modifier will be employed. Rubber toughening is one of the traditional approaches to improve toughness in brittle polymers consisting in the incorporation of a secondary dispersed elastomeric phase that acts as an impact modifier increasing the impact-absorbed energy of the resin.[9] This strategy has been recently applied in PHBV matrices using ethylene–vinyl acetate,[10] epoxidized natural rubber,[11,12]

poly(butadiene-*co*-acrylonitrile),[13] or thermoplastic polyurethane (TPU)[14,15] as the secondary elastomeric phase showing improvements in elongation at break and impact strength in different extents. In this work, an ester-based TPU was studied as elastomer. The use of a TPU in a PHBV matrix has been previously studied by our group showing a great improvement in toughness maintaining the biodisintegrability in standard composting conditions of the final systems.[16,17] The addition of an elastomeric phase could lead to a reduction in the rigidity and the HDT of the system. That is why, the incorporation of a cheap reinforcing material such as cellulose could counterbalance this and contribute to the reduction of the final costs, preserving the sustainability of the final product.[18] The reinforcing material selected for the present study is a commercial purified alpha cellulose that has demonstrated its efficiency in this system.[19]

Thus, the purpose of this study is to verify that by making ternary blends based in PHBV with an impact modifier and a mechanical reinforcement component (TPU and cellulose in this case, respectively), the industrial applicability of PHBV in rigid part applications can be improved, even without the need of additional compatibilizers.

One issue that is commonly faced in polymer processing is the fact that the processing laboratory techniques (cast solvent, internal mixers, mini-extruders, etc.), like the ones used in the aforementioned earlier studies differ from the typical equipment used in industry, thus leading to different product properties. Therefore, in agreement with the objective of this work, all compounds were processed using conventional pilot plant scale and production-like conditions. Likewise, all the raw materials were chosen to be available commercially at large scale, so conclusions can be directly forwarded to industry.

EXPERIMENTAL

Materials

PHBV commercial grade with 3 wt % valerate content was purchased from Tianan Biologic Material Co. (Ningbo, P.R. China) in pellet form (ENMAT Y1000P). TPU Elastollan 890 A 10FC was supplied by BASF (Germany). Purified alpha-cellulose fiber grade (TC90) from CreaFill Fibers Corp. (Chestertown, MD) was used. According to the manufacturer's specifications, these fibers have an average fiber length of 60 μm and an average fiber width up to 20 μm. The alpha-cellulose content is >99.5%.

Sample Preparation

Before mixing, the three materials were dried. The PHBV and the TPU were dried at 80 °C for at least 6 h in a DESTA DS06 HT Dehumidifier, whereas cellulose fibers were dried in laboratory oven (Memmert Universal Oven U) at 90 °C for a minimum of 16 h.

PHBV/TPU/cellulose blends (systems were prepared in a Labtech LTE (Ø = 26 mm, *L/D* ratio = 40) corotating twin-screw extruder with a temperature profile from hopper to nozzle of 145/155/160/170 °C and 250 rpm rotation speed. This profile is the one usually recommended for neat PHBV and all compounds were processed keeping the same conditions. All the components were manually premixed before extrusion (dry-blend) and fed to the main hopper by the extruder feeder at a speed of about 5 kg h^{-1}. The extruded material was cooled in a water batch and pelletized.

Material pellets were dry again 80 °C for 8 h (DESTA DS06 HT) before injection process. Standardized tensile specimens (ISO-527 Type 1A) were injection molded in a DEMAG IntElect 100 T injection molding machine (two-cavity mold), with an injection temperature of 185 °C at the nozzle. For neat PHBV, a holding pressure of 600 bar was applied for 12 s, followed by 40 s of cooling time, being the mold temperature set at 60 °C. The same injection conditions were used for the rest of the compounds.

For the sake of comparison, neat PHBV was also processed under identical conditions to those of the different blends and composites.

Prior to any characterization, all the samples were annealed at 80 °C for 48 days in order to obtain equivalent crystallinity and mechanical performance to aged samples.

Samples are named as X/Y/Z in the order PHBV/TPU/cellulose were X, Y, and Z are the content of each component. The content of the additives TPU and cellulose is expressed in phr referred to 100% PHBV matrix. As an example, the sample 100/30/10 corresponds to a weight ratio of 100 g PHBV with 30 g TPU and 10 g cellulose. Table I summarizes the compositions studied.

Characterization

The melt flow index (MFI) of the neat polymers and the different compounds was measured in a Tinius Olsen MP600 melt flow indexer according to ISO 1133 standard. The tests were performed at 185 °C and 2.16 kg load.

Morphology of cellulose, neat PHBV, as well as the compounds were examined by scanning electron microscopy (SEM) using a high-resolution field-emission JEOL 7001F microscope. The fracture surfaces from impact-fractured specimens were coated by sputtering with a thin layer of Pt prior to SEM analysis. The size distribution of the dispersed phase of the blends was evaluated with ImageJ software (the number of spheres measured was in all cases >600).

Tensile tests were conducted on ISO-527 Type 1A injection molded specimens in a universal testing machine Hounsfield H25K equipped with a 25 kN load cell according to ISO-527-1:2012 standard.

Notched and unnotched Charpy impact tests were carried out by means of an ATS Faar IMPats-15 impact pendulum with a 4J hammer according to ISO 179 standard. Samples were cut form injection molded bars.

Table I. Compositions Studied

Sample PHBV/TPU/cellulose (phr)	PHBV (wt %)	TPU (wt %)	Cellulose (wt %)
100/0/0	100	-	-
100/10/0	90.9	9.1	-
100/30/0	76.9	23.1	-
100/0/10	90.9	-	9.1
100/0/30	76.9	-	23.1
100/10/10	83.3	8.3	8.3
100/10/30	71.4	7.2	21.4
100/30/10	71.4	21.4	7.2
100/30/30	62.5	18.7	18.7

Shore D hardness of the obtained blends and composites was measured in a Zwick 3100 Shore D tester (Zwick GmbH, Germany).

Differential scanning calorimetry (DSC) experiments were conducted on a TA Instruments Q100 model calibrated with Indium and sapphire standards before use. Samples with a typical weight of 6–8 mg were obtained from injection molded specimens. Samples were first heated from −40 to 210 °C at 10 °C min^{-1} and maintained 2 min to erase thermal history, cooled down to −40 °C and subsequently heated to 210 °C at 10 °C min^{-1}. Melting temperatures (T_m) and enthalpies (ΔH_m), as well as crystallization temperatures (T_c), and enthalpies (ΔH_c), were calculated from the second heating and cooling curves, respectively. The crystallinity (X_c) of the PHBV phase of blends and composites was determined by applying the following expression[20]:

$$X_c(\%) = \frac{\Delta H_m}{w \cdot \Delta H_m^0} \times 100 \quad (1)$$

where w is the PHBV weight fraction in the blend, ΔH_m (J g^{-1}) is the melting enthalpy of the polymer matrix, and ΔH°_m is the theoretical melting enthalpy of 100% crystalline PHB (perfect crystal) (146 J g^{-1}).[21] This value is considered a good approximation for PHBV due to its low HV content.[22]

Thermogravimetric analysis (TGA) of cellulose, as well as the PHBV, TPU, and the compounds (from injection molded parts), were performed with a TG-STDA METTLER TOLEDO model TGA/STDA851e/LF/1600 analyzer. The samples with an initial mass of typically about 15 mg were heated from 30 to 900 °C at a heating rate of 10 °C min^{-1} under nitrogen flow. The thermal stability of cellulose, neat polymers, and the blends and composites was evaluated and the residue at 900 °C was determined. The onset decomposition temperature ($T_{5\%}$, temperature at 5% weight loss) and the maximum decomposition rate temperature (T_d) were determined from the weight loss curve and the maximum value of weight loss derivative, respectively.

HDT analyses were performed using a Deflex 687-2. A heating rate of 120 °C h^{-1} was used with an applied load of 1.8 MPa in accordance with Method A of ISO 75 standard. Temperature signal was recorded until the sample deflects 0.35 mm.

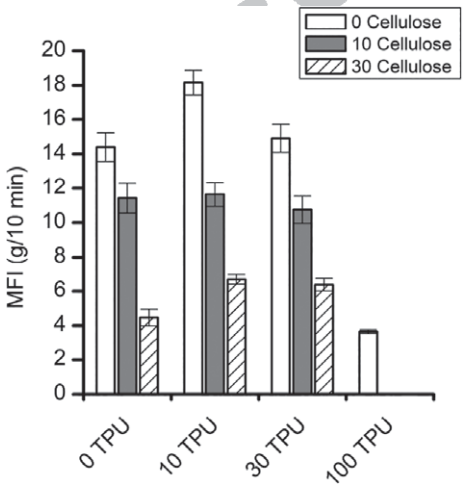

Figure 1. MFI of neat PHBV and TPU and the PHBV/TPU/cellulose compositions.

Disintegration tests were carried out with samples of (15 × 15 × 0.2 mm^3) obtained from hot pressed plates (180 °C, 5 min, and ca. 40 bar). Tests were performed according to the ISO 20200 standard.[23] Solid synthetic waste was prepared by mixing 10% of activated mature compost (Vigorhumus H-00, purchased from Burás Profesional, S.A., Girona, Spain), 40% sawdust, 30% rabbit feed, 10% corn starch, 5% sugar, 4% corn seed oil, and 1% urea. The water content of the mixture was adjusted to 55%. The samples were placed inside mesh bags to simplify their extraction and allow the contact of the compost with the specimens, then buried in compost bioreactors at 4–6 cm depth. Bioreactors were incubated at 58 °C. The aerobic conditions were guaranteed by mixing the synthetic waste periodically and adding water according to the standard requirements. Three replicates of each sample were removed from the boxes at different composting times for analysis. Samples were washed with water and dried under vacuum at 40 °C until a constant mass. The disintegration degree was calculated by normalizing the sample weight to the initial weight with eq. (2):

$$D = \frac{m_i - m_f}{m_i} \times 100 \quad (2)$$

where m_i is the initial dry mass of the test material and m_f is the dry mass of the test material recovered at different incubation stages. The disintegration study was completed by SEM micrographs of the disintegrated surface and by taking photographs for visual evaluation.

RESULTS AND DISCUSSION

Samples Processability

Figure 1 indicates the MFI values for the different blends, neat PHBV (previously processed at the same conditions than the blends to keep the same thermomechanical history) and raw TPU, measured at 185 °C. As a reference, it is considered that a value of MFI of 7 is enough to be able to fill by injection molding process medium to high size parts. Results indicate that in all PHBV compositions the MFI is kept over this value, except on those formulations containing 30 phr cellulose. The addition of 10 phr TPU leads to an increase in the MFI values, but it does not increase any further when it is added at a higher load (30 phr). In any case, the MFI variations are not critical at the processing conditions applied (see the Experimental section). All the compounds have been successfully obtained without needing any modification of the processing parameters and without producing significant degradation from their processability point of view (see the Thermogravimetric Analysis section).

Blends and Composites Morphology

The morphology of the cellulose fibers, the PHBV/TPU, PHBV/cellulose, and PHBV/TPU/cellulose blends has been examined by SEM. The TPU particle size, shape, and their distribution in the blends have been analyzed, being the results summarized in Figure 2 (for both systems, without and with cellulose).

The dominant morphology can be described, in all cases, as a two-phase morphology, revealing an immiscible polymeric system with a characteristic discrete-phase structure (or drop in

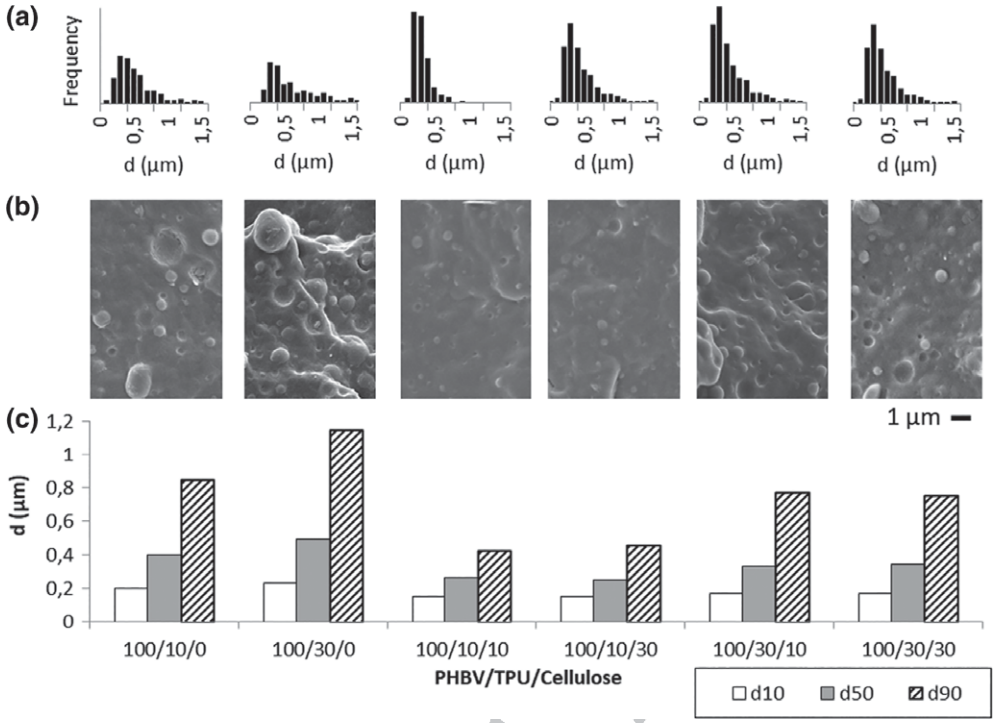

Figure 2. (a) Sphere size frequency histograms; (b) representative micrographs of the drop-in-matrix morphology; and (c) d10, d50, and d90 values of the TPU drops for the PHBV/TPU/cellulose blends.

matrix). The TPU appears as small spherical droplets in all the studied compositions, being homogeneously dispersed into the PHBV matrix. The sphere size frequency histograms, the d10, d50, and d90 values (i.e., the size under which 10, 50, or 90% of the particle distribution, respectively, lies) and representative micrographs are shown in Figure 2.

An increase in the size of the elastomeric droplets as the TPU content is increased is observed. The analysis of the results reveals that the distribution size is wider in the samples with the highest TPU content. The differences in size are principally detected in the d90 value, while d10 and d50 values remain practically unchanged for all the compositions. Hence, a considerable increase of 35% in d90 is found for blends with high TPU content, resulting in droplets with sizes above 1.5 μm. This fact might be ascribed to a coalescence phenomenon due to the low melt viscosity of the PHBV and the higher content or TPU.

The incorporation of the cellulose fibers in PHBV/TPU blends leads to a reduction in the size of the droplet disperse phase. For the sample 100/10/10, the average droplet size is reduced from 0.5 to 0.3 μm with the introduction of 10 phr cellulose, finding a similar value of about 0.3 μm for 100/10/30. However, the most visible change in the droplet size is found for the d90, where a decrease to almost half is detected for both 10 and 30 phr cellulose. A similar trend is also found for the sample with the highest TPU content. The reduction of the sphere size with the incorporation of the fillers can be explained by either the highest melt viscosity of the compositions (according to the lower MFI values, shown in Figure 1), the effect of the fibers limiting the extent of coalescence, the droplet confinement and break due to the presence of fibers or because of the differences in local shearing during processing.

With respect to the interface of the TPU particles in the PHBV matrix, during SEM analysis, it was observed that some of the droplets are partially covered by PHBV, as in Figure 2 (b) 100/30/0 (thus indicating a coherent interface, in agreement with the good distribution of the TPU). However, detachment of the spheres is also detected in all compositions studied. These apparent contradictory observations may have its origin in the mode of failure of the specimens prior to SEM analysis, which were obtained after impact testing, as it will be discussed later on.

With respect to the fillers, Figure 3 presents the SEM micrograph of the cellulose fibers. As shown, the cellulose fibers present a rod-shaped morphology with varying lengths up to 200 μm. The

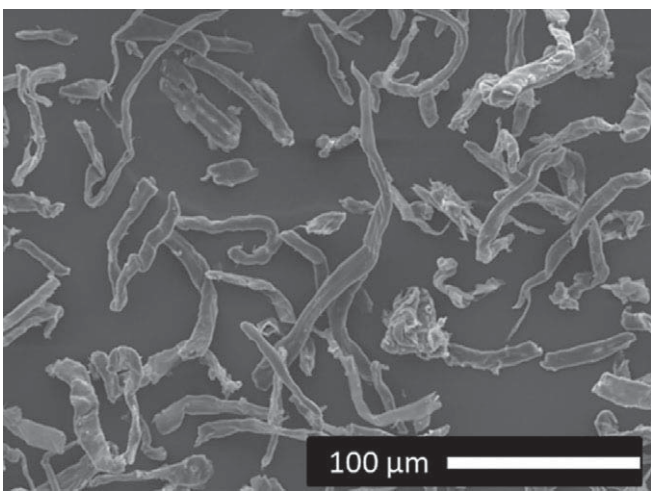

Figure 3. SEM micrograph of cellulose fibers.

diameter of the fibers is in the 5–20 μm range and their average aspect ratio is of about 10. Figure 4 presents the morphology of the impact-fractured surfaces of different compounds.

Figure 4(a,b) shows the representative low magnification images corresponding to PHBV/Cellulose composites with 10 and 30 phr cellulose content, respectively, and a detail of the fiber/matrix interface. Even at high cellulose content formulations, homogeneous distribution of the fibers was observed. The presence of fiber aggregates has not been detected and the individual fibers appear homogeneously distributed throughout the polymer matrix, thus confirming that an effective compounding has been achieved. Similar trend was observed in PHBV/TPU/cellulose composites. In order to analyze the interaction between the polymer and the cellulose fibers, high magnification micrographs of all PHBV/cellulose and PHBV/TPU/cellulose composites were used [Figure 4(c–f)]. Broken fibers have been detected in all compositions, thus revealing some degree of interaction between the cellulose and the biopolyesters. This is in agreement with previous results[19] and could be attributed to the formation of a hydrogen-bonding-type interaction between carbonyl groups of PHBV and hydroxyl groups of the cellulose.[24] However, when analyzing the interphase, as for the TPU second phase, some detachment is also detected at some point, revealing a weak interphase interaction.

Mechanical Properties

The mechanical properties of the neat PHBV and the blends with TPU and cellulose have been evaluated by tensile tests up to failure. Young's modulus, maximum tensile strength, and elongation at break of all compositions are gathered in Figure 5. A representative stress–strain curve of neat PHBV and the blends containing the highest amount of TPU and/or cellulose (30 phr), is also depicted in Figure 5(d) for clarification.

As it could be expected, the incorporation of TPU resulted in a reduction in the rigidity and tensile strength of the blend, along with an increase in the elongation at break and tensile static toughness, estimated from the area under the stress–strain curves [Figure 6(c)]. Thus, the tensile modulus of elasticity decreased from about 3.4 GPa

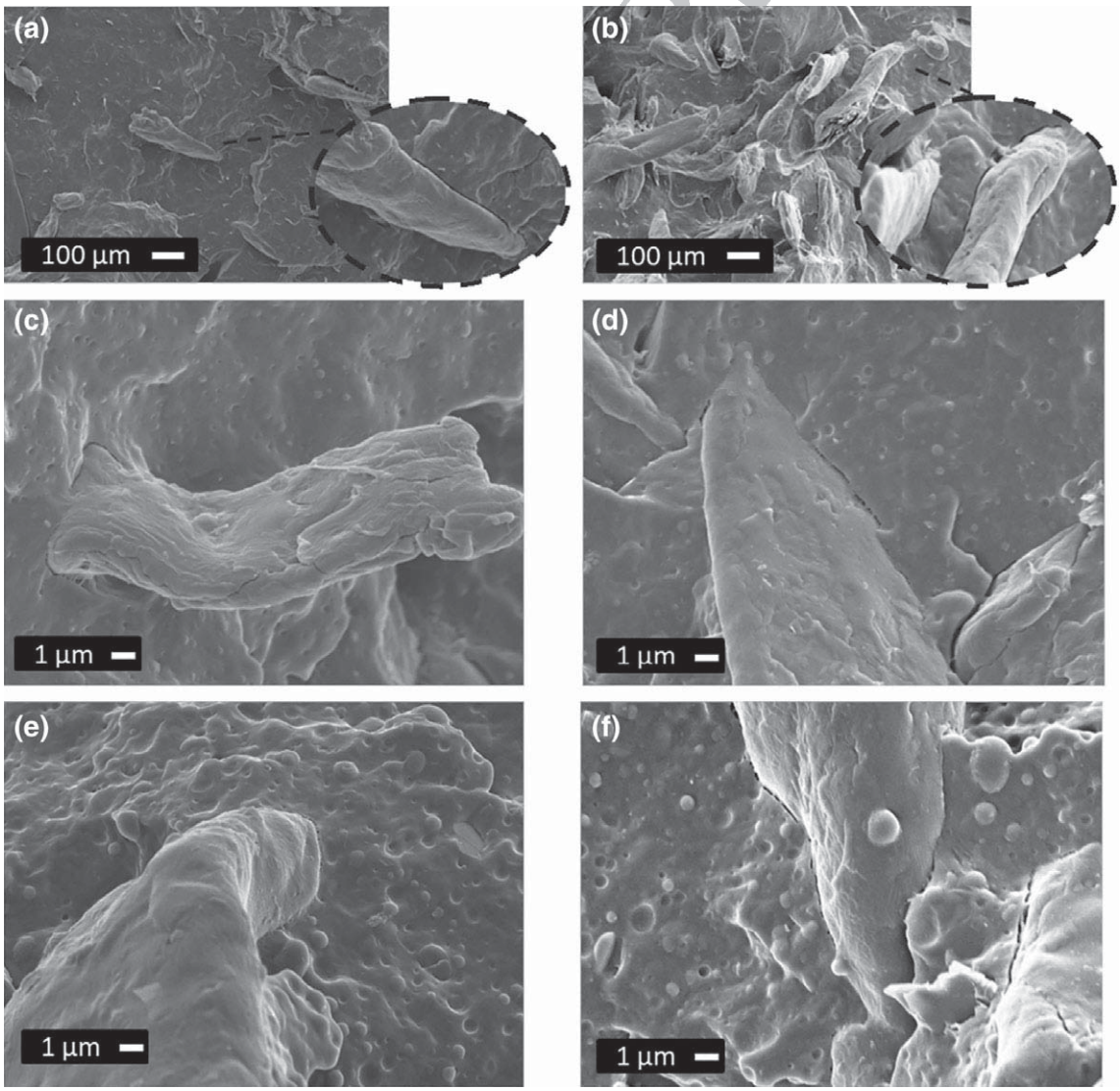

Figure 4. SEM micrographs of PHBV/TPU/cellulose blends: (a) 100/0/10, (b) 100/0/30, (c) 100/10/10, (d) 100/10/30, (e) 100/30/10, and (f) 100/30/30.

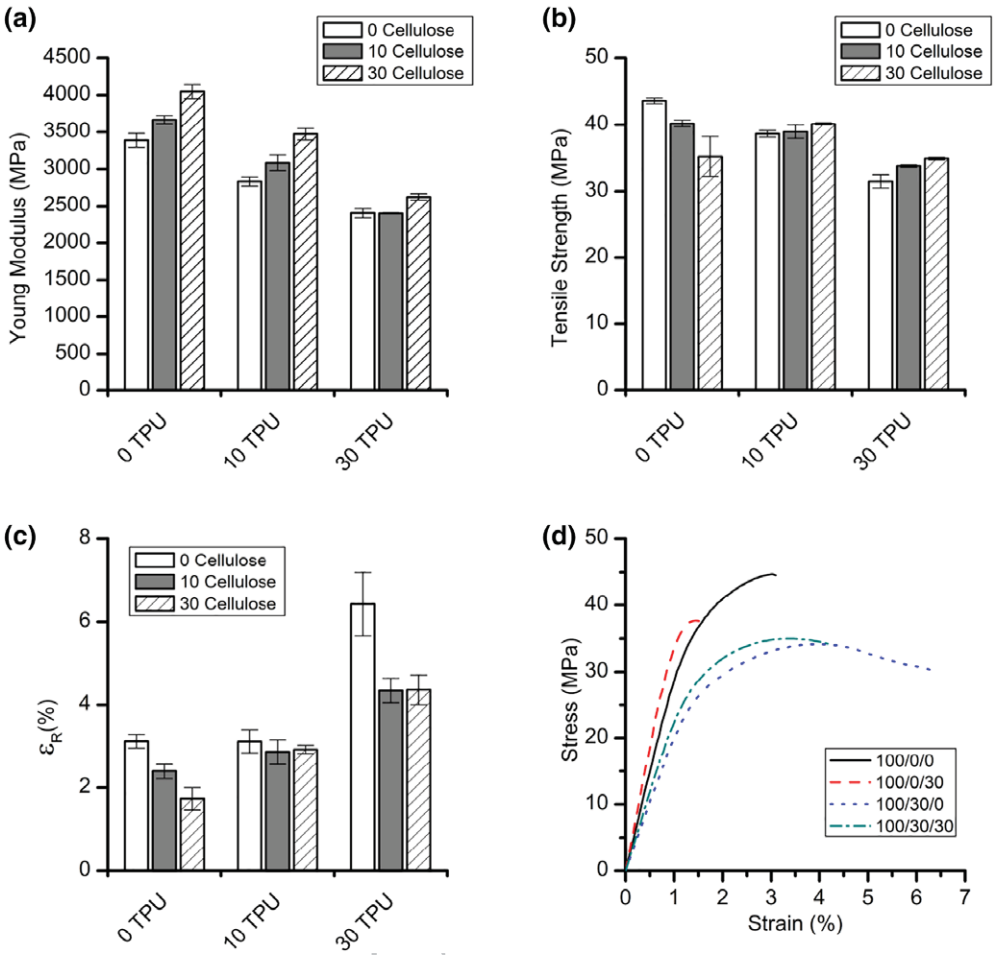

Color online, B&W in print

Figure 5. Mechanical properties of the neat PHBV and PHBV/TPU/cellulose blends. (a) Young's modulus, (b) tensile strength, (c) elongation at break, and (d) representative stress–strain curves of neat PHBV and the binary and ternary systems containing the highest amount of additives TPU and/or cellulose (30 phr). [Color figure can be viewed at wileyonlinelibrary.com]

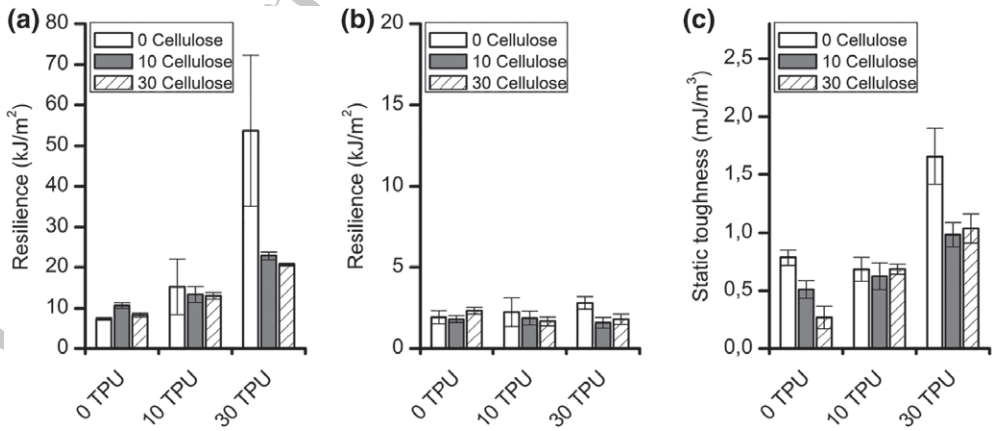

Figure 6. Charpy impact results for (a) unnotched specimens, (b) notched specimens, and (c) static toughness from the area below the strain–stress curve.

for pristine PHBV to about 2.5 GPa for the highest TPU content blend, the decrease being dependent on the TPU content. On the other hand, the incorporation of 30 phr TPU supposed an increment of the elongation at break of 105% with respect to neat PHBV. This improvement is in accordance with other works reported in the literature of PHBV/TPU blends with the same range of composition.[17,25]

With respect to the static toughness, the TPU has a clear toughening effect resulting in almost a twofold increase in the area beneath the stress–strain curve.

On the contrary, the incorporation of the cellulose fibers to the PHBV matrix results in an increase of Young's modulus, showing

a reinforcing effect, positively dependent upon the filler content. Concurrently, a reduction of the elongation-at-break and the static toughness with the cellulose content is also registered, thus revealing an embrittlement of the samples. The reduction in the ductility of the compound is such that the breaking takes place before yielding and, consequently, the tensile strength is also reduced with the incorporation of the fiber. This embrittlement can be explained in terms of a limited interaction between the fibers and the matrix. At small deformations, there is a positive reinforcement effect, with an increase in elastic modulus. However, once the strain overcomes a certain value, within the elastic deformation range, a detachment of the fiber occurs generating a void between the fiber and the polymer matrix, a flaw that can easily act as crack initiator, causing premature material failure.[12,26] Once the crack is nucleated, its propagation is straightforward throughout the PHBV matrix due to its intrinsic fragility.

The incorporation of cellulose fibers to PHBV/10TPU blends, thus obtaining the 100/10/10 and 100/10/30 ternary systems, produces an increase in Young's modulus and tensile strength with respect to the unfilled blend, whereas their values of elongation at break remain practically unchanged. It is interesting to note that the composition 100/10/30 present similar overall mechanical properties than neat PHBV. With respect to the highest TPU content blends, the incorporation of the cellulose fibers did not result in a significant increase in Young's modulus or tensile strength, while yielding in a reduction in elongation at break with respect to unfilled blends. However, when compared to the neat PHBV, there is a reduction in rigidity (ca. 25%) but an enhancement in elongation at break (ca. 40%) and static toughness (25 and 32% for the 10 and 30 phr cellulose, respectively).

Impact Test

One of the key limitations for the use of PHBV for injection molded rigid parts is its relative low toughness when compared to oil-based counterparts (i.e., ABS and PP). The strategy considered in the present work is the addition of an ester-based biodegradable TPU as impact modifier. Notched and unnotched Charpy impact tests were conducted on PHBV, PHBV/TPU, and cellulose-containing blends. The results of Charpy impact tests and the static toughness (as obtained from the area below the strain–stress curve) are summarized in Figure 6.

From the data shown in Figure 6(a), it can be deduced that the incorporation of TPU to the PHBV enhances the capacity of the blends to absorb impact energy. Hence, the resilience increase with the incorporation of the elastomer rises from 7.38 to 10.64 kJ m^{-2} for 10 phr TPU content and further up to 53.71 kJ m^{-2} for 30 phr TPU content. This trend is in agreement with the improvement in the static toughness, as obtained by tensile tests [Figure 6(c)]. The good dispersion of the elastomeric phase in the PHBV observed in SEM images [Figure 2(b)] could be responsible for the good delivery of the stress and thus the enhancement of toughness.[25]

However, the resilience values for the notched specimens are way below the unnotched ones; for instance, when comparing the neat PHBV with and without notch, the difference is of an order of magnitude. This evidences that the presence of a flaw (by means of the notch) plays a critical role in the impact strength of these materials. This behavior can be attributed to the intrinsic fragility of the PHBV (i.e., low tolerance to the presence of flaws), in the way that the crack propagation takes place without noticeable yielding of the matrix. For the notched compositions incorporating TPU, the toughening effect does not seem to be as effective as for the unnotched ones; thus, confirming the crack preferential propagation pathway throughout the PHBV matrix. Moreover, attending to the SEM micrographs of the impact-fractured surfaces of the polymer blends (shown in Figure 2), the propagation of the crack occurs across the PHBV and through the TPU PHBV interphase, resulting in the observed detachment of the TPU particles. This fact evidences that the interfacial adhesion between both polymers is not very strong, limiting the reinforcement ability of the elastomeric phase when stress raisers, such as notches, are present in the samples.

The incorporation of the cellulose to the pure PHBV did not affect significantly the resilience of the polymer regardless the filler content, whether the tests were conducted with or without notch. For the ternary compounds, the toughening effect of the TPU is partially compromised by the presence of the cellulose, being this effect more remarkable for those with 30 phr TPU. The reason behind this trend can be found in the detachment of the cellulose fibers during elastic deformation, which may act as flaws, as previously discussed in the mechanical properties section.

Hardness

Shore D hardness of neat PHBV and the developed compounds has been assessed. The results (summarized in Table II) are in accordance with the rigidity of the different compositions, that is, a decrease with the incorporation of the TPU and a reinforcing effect provided by the cellulose.

DIFFERENTIAL SCANNING CALORIMETRY

The thermal behavior of neat PHBV and the prepared blends is studied by DSC. The melting and crystallization enthalpies (ΔH_m and ΔH_c), characteristic temperatures (T_m and T_c), and the crystallinity (X_c) are summarized in Table III.

DSC results reveal that the addition of TPU to PHBV produces a slight decrease in both crystallinity and melting and crystallization temperatures of the blends in the composition range studied

Table II. Shore D Hardness of the Studied Compositions

PHBV/TPU/cellulose	Shore D	SD
100/0/0	81.3	1.0
100/10/0	77.9	1.4
100/30/0	75.6	1.1
100/0/10	83.4	1.3
100/0/30	84.4	1.1
100/10/10	80.7	0.9
100/10/30	82.5	0.5
100/30/10	75.6	1.2
100/30/30	78.6	1.6

Table III. DSC Data of PHBV/TPU/Cellulose Compounds

	DSC parameters				
PHBV/TPU/cellulose	ΔH_m (J g^{-1})	T_m (°C)	ΔH_c (J g^{-1})	T_c (°C)	X_c (%)
100/0/0	94.1	173.9	86.7	119.4	64.5
100/10/0	80.8	171.2	74.8	110.3	60.9
100/30/0	67.2	170.2	61.9	105.6	59.9
100/0/10	85.4	173.8	77.9	121.1	64.4
100/0/30	74.6	172.7	67.9	119.9	66.4
100/10/10	75.8	173.5	70.7	111.5	62.4
100/10/30	66.3	172.4	60.8	109.6	63.7
100/30/10	61.5	169.7	56.5	107.0	59.0
100/30/30	57.8	170.9	53.3	107.0	63.4

indicating that this component affects the crystallization process. These findings are in accordance with the previous works about PHBV/TPU blends reported in literature.[15,17,25] Such behavior can be explained by the intermolecular interactions (i.e., dipole–dipole) between the phases in the liquid state, introducing some disorder in the system, which would be hampering the crystallization. Once crystallization takes place, the TPU phase is excluded from the crystals, giving a final completely segregated morphology. The addition of 10 phr cellulose content to PHBV practically does not change neither the crystallization/melting temperatures nor the crystallinity index. A minimum increase in crystallinity has been found for the highest filler content (100/0/30) with respect to neat PHBV and in the ternary systems with respect to the unfilled PHBV/TPU compositions. However, in agreement with other studies, such small differences in crystallinity are not attributed to a nucleating effect of the cellulose.[19,27–29]

THERMOGRAVIMETRIC ANALYSIS

The thermal degradation behavior of neat PHBV, TPU, cellulose, and their compounds was studied by TGA. The TGA and their first derivatives curves are depicted in Figure 7. The onset degradation temperature ($T_{5\%}$), the maximum degradation temperature (T_d), and the weight residue at 600 °C are summarized in Table IV.

As it is well reported, PHBV thermal degradation takes place abruptly in a single weight loss step by the chain scission reaction mechanism[30] with an onset at 279 °C and the maximum degradation temperature at 299 °C. Cellulose thermal degradation also takes place in a single weight loss step around 347 °C, with a residue of 14.47% at 600 °C, in agreement with previous works.[19,31] Thermal degradation of TPU occurs between 300 and 450 °C with a residual weight of about 6.5% at 600 °C. TPU–DTG curve presents two peaks at 368 and 389 °C and a shoulder at around 425 °C. The first step of degradation is attributed to the scission of the urethane bond and to the release of the smaller molecules or unstable side chains followed by the chain scission at the β-position to the carbon–carbon double bond.[32,33]

PHBV/TPU blends showed two degradation stages, of which the first stage was ascribed to the PHBV degradation while the second stage was from TPU degradation. The onset and maximum degradation temperatures of the blends with 10 and 30 phr TPU content are comparable to those corresponding to neat PHBV indicating that the presence of this component does not affect

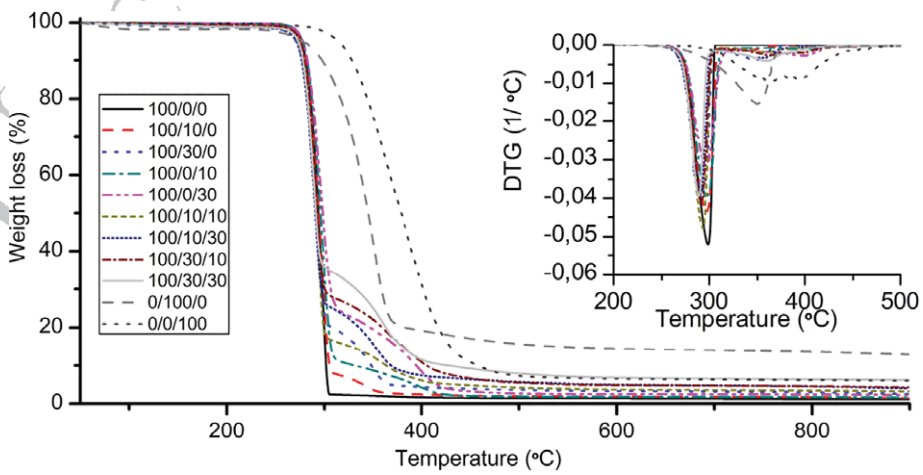

Color online, B&W in print

Figure 7. TGA and DTG (inset) curves of neat PHBV, TPU, and cellulose and PHBV/TPU/cellulose systems. [Color figure can be viewed at wileyonlinelibrary.com]

Table IV. TGA Data of PHBV/TPU/Cellulose Compounds

	TGA parameters		
PHBV/TPU/cellulose	$T_{5\%}$ (°C)	T_d (°C)	Residue at 600 °C (%)
100/0/0	279	299	1.4
100/10/0	278	297	1.8
100/30/0	278	295	2.5
100/0/10	276	297	1.9
100/0/30	271	291	3.3
100/10/10	275	294	3.7
100/10/30	271	290	5.0
100/30/10	276	291	4.9
100/30/30	273	289	6.8
0/100/0	315	385	6.6
0/0/100	278	347	14.5

the thermal stability of PHBV, as it has been previously reported.[17] PHBV/cellulose and PHBV/TPU/cellulose compounds present two and three degradation steps, respectively, according to the decomposition of their respective components. The incorporation of the cellulose fibers slightly decreases both the onset and maximum degradation temperatures, especially for the highest cellulose content (30 phr), in agreement with others works.[19,34]

HEAT DEFLECTION TEMPERATURE

HDT represents the temperature at which the material losses its bearing load capacity and is a good parameter to predict the thermal resistance and dimensional stability of the materials in service. Figure 8 shows the HDT-A of neat PHBV and the developed blends and composites.

Neat PHBV presents a HDT-A at 108 °C. Cellulose addition improves this value up to 126 °C for the highest content. Similar results were found in bibliography for neat PHBV and lignocellulosic-based composites.[26,35,36] The improvement in HDT-A with the cellulose addition could be explained by the reinforcing effect induced by the fibers. Also, the increased crystallinity observed by the nucleating effect of the fibers may contribute to rise the HDT-A of the composites.[12,35] On the contrary, TPU incorporation produces a decrease of the HDT-A. Nevertheless, in spite of the negative impact of TPU in the thermal resistance of PHBV, the HDT-A remains in interesting values beyond 90 °C, and the incorporation of the cellulose to PHBV/TPU blends allows almost recover the HDT-A values to that of the neat PHBV. It is interesting to note that the thermal resistance of the blends and composites obtained is really superior to that corresponding to other common biopolymers (e.g., the HDT-A of amorphous poly(lactic acid), the main competitor of PHBV, is of about 55 °C[37]).

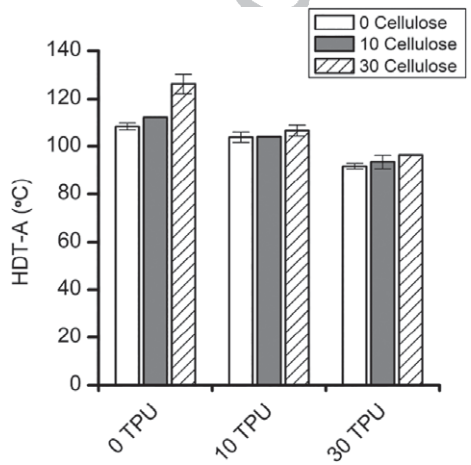

Figure 8. HDT-A of neat PHBV and the PHBV/TPU/cellulose blends.

DISINTEGRABILITY IN COMPOSTING CONDITIONS

PHBV and PHBV/TPU/cellulose disintegration in composting conditions was evaluated according to the ISO 20200 standard. The disintegration rate was determined by measuring the weight loss of the samples as a function of composting time. Results are represented in Figure 9.

No appreciable weight loss was detected for any sample until the 28th day of composting, thus revealing an induction period for the disintegration to take place. From that day onward, no differences in the biodisintegrability behavior (i.e., full biodisintegration achieved before 40 days in agreement with literature reports[17]) has been detected in the studied samples with the exception of the ternary blends containing 30 phr cellulose. No slowdown on the biodisintegration rate was found for the TPU containing samples regardless the slower biodegradation rate of the TPU under composting conditions when compared to PHBV or cellulose.[17,38,39] For the samples containing 30 phr cellulose, a disintegration level around 60–70% was reached at 30 days of composting (corresponding to approximately the PHBV content in the sample). At this point, the weight loss remains practically constant until 50 days of composting. Thus, in the last stage, the disintegration rate increases to achieve total disintegration at 73 and 90 days for the compositions containing 10 and 30 phr TPU, respectively. The slower biodisintegration rate of the high cellulose content composition may be seemed as counterintuitive

(being the cellulose known as an easy biodegradable material); nevertheless, the reason behind this behavior could be related to a formation of a percolative structure of cellulose fibers together with the TPU that hinders the biodisintegration. The biodisintegration process starts from the surface[40–42] and advances primarily through the PHBV phase, thus leaving an interconnected fiber/TPU structure (see Figure 10).

Photographs at different composting times were taken in order to assess the impact of composting process on the tested samples. The photographs are shown in Figure 11.

Considerable surface erosion and fractures are found after 28 days in composting and after 35 days the samples are broken into small pieces, except for the triple systems 100/10/30 and 100/30/30. As it has been discussed previously, the particular morphology of these samples causes a slowing down of the disintegration rate. For these samples, although color changes are detected from 35 days in compost, no clear surface damage is observed until 47 days of composting where disintegration rates increases.

Except for the 100/10/30 and 100/30/30 systems, the rates and time periods of disintegration of the studied samples are within the same range of the values reported in literature for different PHA based materials.[17,41–44] In addition, regardless of the rate of disintegration, all systems have reached more than 90% disintegration within the period of time established in ISO 20200, so they can be considered biodisintegrable under composting conditions.

General Discussion

When considering as a whole the data showed in the present work, it becomes clear the influence of each component in the studied compounds. First, the PHBV and the TPU show some degree of affinity between them. This is evidenced by the fact that there is a good dispersion of small droplets of TPU within the matrix; indeed, the MFI of the PHBV/TPU blends increases with

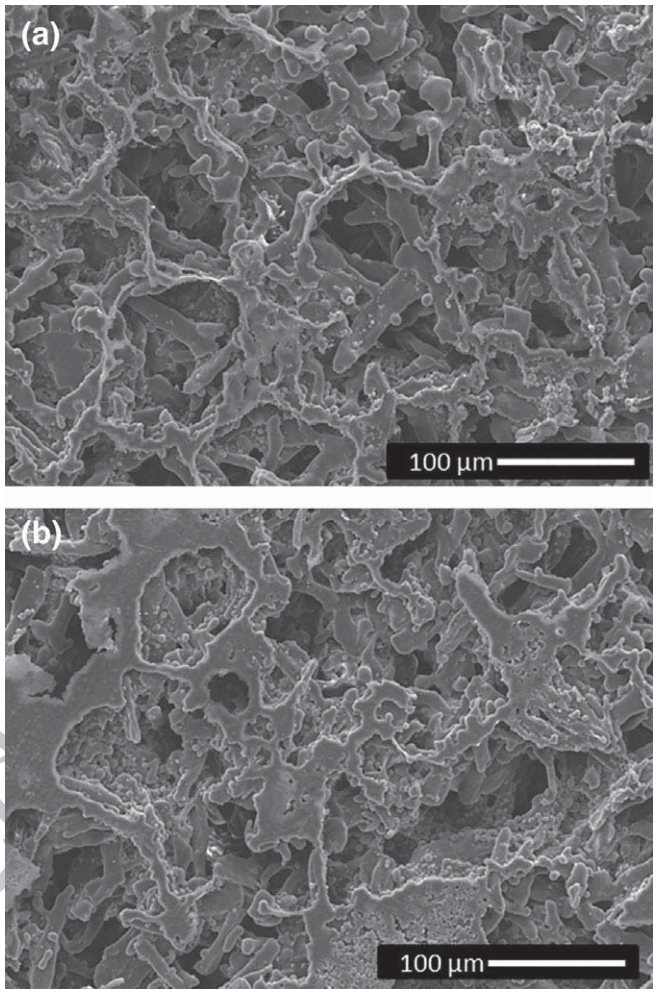

Figure 10. SEM micrographs of the samples (a) 100/10/30 and (b) 100/30/30 at 47 days of composting test.

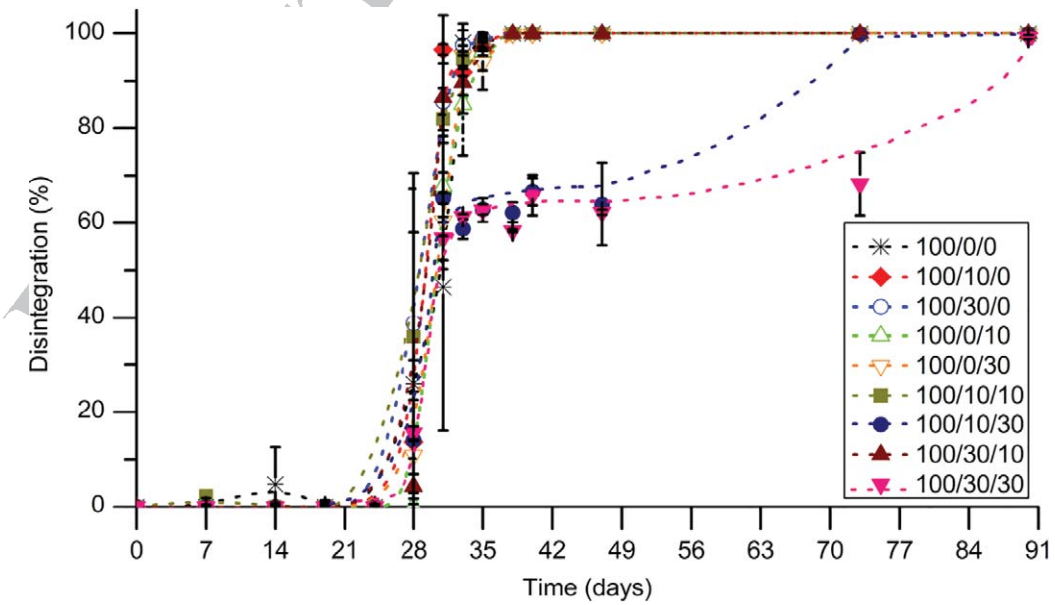

Color online, B&W in print

Figure 9. Disintegration of neat PHBV and PHB/TPU/cellulose systems over time under composting conditions. [Color figure can be viewed at wileyonlinelibrary.com]

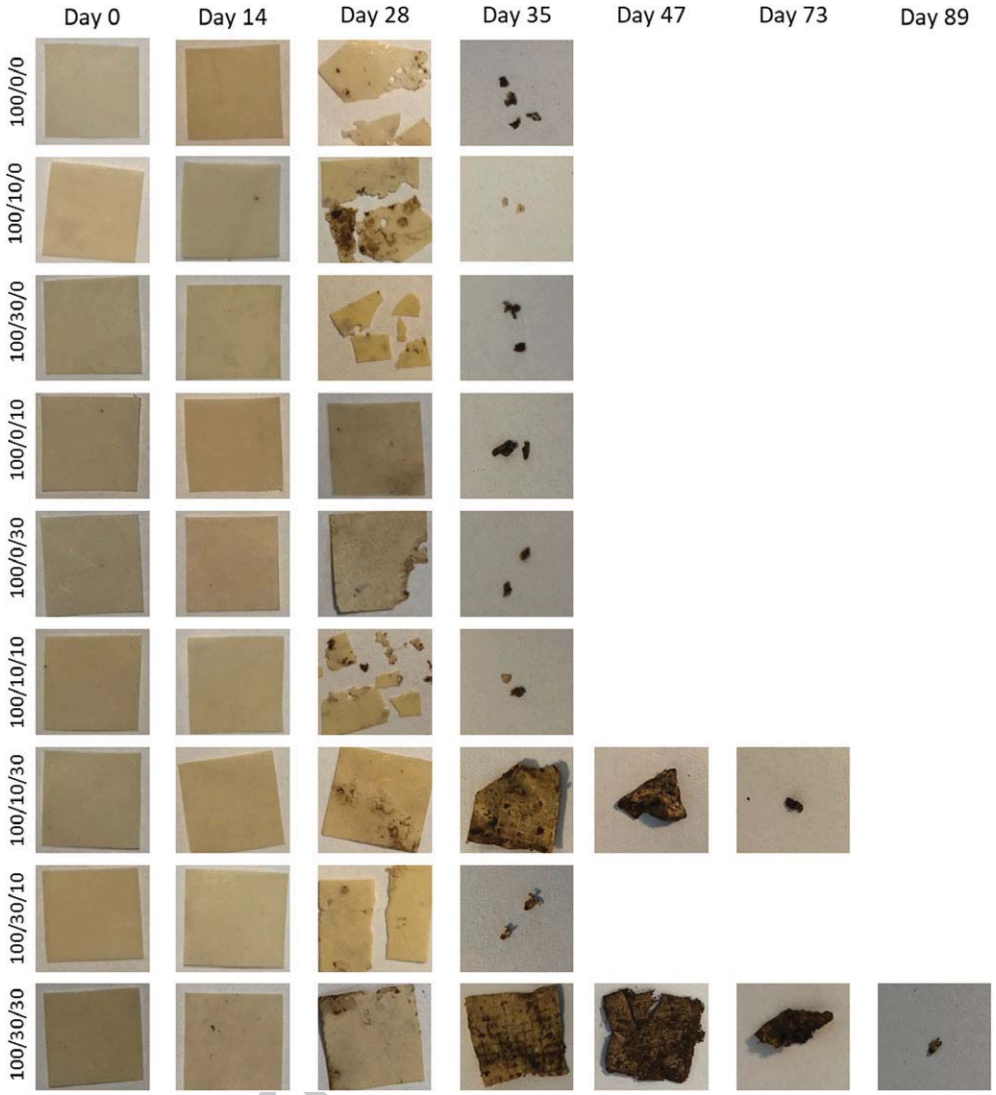

Color online, B&W in print

Figure 11. Photographs of the studied samples at different composting times. [Color figure can be viewed at wileyonlinelibrary.com]

respect to the original constituents. Discarding degradation and in agreement with the small size of the droplets, this type of behavior in melt viscosity of blends is typical of compatible, well-dispersed systems submitted to low constant shear rates. This phenomenon is attributed to the low surface tension between the polymer phases, which enhances the flowability of the blend and therefore reduces its viscosity.[45,46] Indeed, this type of affinity is also supported by PHBV covering TPU droplets and by DSC thermograms, where crystallization is hampered by the TPU.

The mechanical properties of the blends are in agreement with this type of affinity, showing a decrease in elastic modulus and tensile stress, but higher deformation at break as the TPU fraction increases.[17] At high strain rates, such as in impact tests, TPU promotes plastic deformation thus enhancing the toughness of the blends with respect to neat PHBV. HDT values and hardness decrease with respect to PHBV, as one may expect by adding an elastomeric phase to a rigid polymer matrix.

Similarly, some chemical affinity between the PHBV matrix and the cellulose fibers can also be deduced by the good distributive dispersion of the cellulose within the matrix along with the observed polymer covering the fibers in SEM microscopy (as in Figure 4). The tensile properties also reflect this interaction between the PHBV and the cellulose, showing an increase in the elastic modulus. However, the nature of this adhesive interaction does not seem to be very strong, since the reinforcement effect does not withstand the elastic deformation of the matrix. The shear forces between PHBV and cellulose fibers during the tensile stress generate decohesion, resulting in flaws that initiate the crack propagation. The result is that despite of the sticky interaction between the matrix and the reinforcement, there is no increase in tensile strength or toughness. At impact rates, the performance of the composite is ruled by the matrix, but hardness and HDT are increased by the cellulose fibers.

When the compounds include both TPU and cellulose fibers, the reinforcement effect of the fibers is compensated by the softening effect of the TPU, finding some interesting combination of properties. Some compounds like 100/10/30 showed increased unnotched toughness, high HDT, and similar values of elastic

modulus and tensile strength as neat PHBV, but with the potential reduction in cost that implies the introduction of a cheaper filler as is the cellulose. We consider that the PHBV affinity with TPU and cellulose is much higher in molten state than once PHBV has crystallized, since carbonyl groups of PHBV are more exposed in its amorphous state and can interact with polar groups of TPU and cellulose. That explains the increase in elastic modulus and good phase dispersion, but the lack of effective reinforcement in tensile strength, which is dominated by the PHBV matrix.

Regarding the stability of the compounds, TGA analysis show that these are practically as stable as pristine PHBV, except for those containing 30 phr cellulose. For those compounds, the thermal degradation temperature was slightly reduced. Nevertheless, it is worthwhile noticing that in those cases, the onset and maximum degradation temperatures remain in values above the typical processing temperatures, so the decrease of thermal stability does not have a big impact on the overall performance of the composites. When they are tested under ISO 20200 biodisintegration tests, the samples with TPU and high cellulose content did show an unexpected low biodisintegration rate. This phenomenon was explained by the fact that the cellulose can make a mesh and as the PHBV matrix is rapidly bio assimilated, the TPU particles, which biodegrade at lower rates, coalesce on top of the fibers, thus making a net of cellulose where microorganisms cannot easily access. Once the microorganisms reach the cellulose, the disintegration proceeds at the expected high rate.

CONCLUSIONS

In this work, PHBV compounds with an elastomeric phase (TPU) and cellulose fibers as reinforcement have been proved a technical reasonably good environmental friendly alternative to nonbiodegradable oil based polymers for injection molding applications.

The results show a homogeneous distribution of the TPU and cellulose, well dispersed within the PHBV matrix. The fairly good affinity between PHBV and TPU and between PHBV and cellulose indicated that these systems might be compatible enough to be processed without any compatibilization agents.

TPU promotes plastic deformation and an increase in toughness, whereas cellulose increases the elastic modulus but yields premature break of the composites. Thus, adding cellulose to PHBV/TPU blends counteracts some of the loss of mechanical performance but maintaining the toughness improvements ascribed to TPU.

Despite the affinity between the matrix and dispersed phases, the failure of the compounds was triggered by the limited bond strength at the interface of PHBV with the other phases.

ACKNOWLEDGMENTS

The authors would like to thank the financial support for this research from Ministerio de Economia y Competitividad (AGL2015-63855-C2-2-R) and Pla de Promoció de la Investigació de la Universitat Jaume I (UJI-B2016-35). The authors would also like to acknowledge Servicios Centrales de Instrumentación (SCIC) of Universitat Jaume I for the use of TGA and SEM. The authors are also grateful to Raquel Oliver and Jose Ortega for their experimental support.

REFERENCES

1. Nakajima, H.; Dijkstra, P.; Loos, K. *Polymers.* **2017**, *9*, 523.
2. Peelman, N.; Ragaert, P.; Ragaert, K.; De Meulenaer, B.; Devlieghere, F.; Cardon, L. *J. Appl. Polym. Sci.* **2015**, *132*, n/a.
3. Laycock, B.; Halley, P.; Pratt, S.; Werker, A.; Lant, P. *Prog. Polym. Sci.* **2013**, *38*, 536.
4. Albuquerque, P. B. S.; Malafaia, C. B. *Int. J. Biol. Macromol.* **2018**, *107*, 615.
5. Wang, Y.; Yin, J.; Chen, G. Q. *Curr. Opin. Biotechnol.* **2014**, *30*, 59.
6. Pilla, S. Handbook of Bioplastics and Biocomposites Engineering Applications; **2011**.
7. Keskin, G.; Kızıl, G.; Bechelany, M.; Pochat-Bohatier, C.; Öner, M. *Pure Appl. Chem.* **2017**, *89*, 1841.
8. Bugnicourt, E.; Cinelli, P.; Lazzeri, A.; Alvarez, V. *Express Polym. Lett.* **2014**, *8*, 791.
9. Bragaw, C. G. **1971**; p 86.
10. El-Taweel, S. H.; Khater, M. *J. Macromol. Sci. Part B: Phys.* **2015**, *54*, 1225.
11. Adams, B.; Abdelwahab, M.; Misra, M.; Mohanty, A. K. *J. Polym. Environ.* **2017**, *1*.
12. Zhang, K.; Misra, M.; Mohanty, A. K. *ACS Sustain. Chem. Eng.* **2014**, *2*, 2345.
13. Park, E.-S.; Kim, H. K.; Shim, J. H.; Kim, H. S.; Jang, L. W.; Yoon, J.-S. *J. Appl. Polym. Sci.* **2004**, *92*, 3508.
14. Wang, S.; Chen, W.; Xiang, H.; Yang, J.; Zhou, Z.; Zhu, M. *Polymers.* **2016**, *8*, 273.
15. Jost, V.; Miesbauer, O. *J. Appl. Polym. Sci.* **2018**, *135*, 46153.
16. González-Ausejo, J.; Sánchez-Safont, E.; Cabedo, L.; Gamez-Perez, J. *J. Multiscale Model.* **2016**, *7*, 1640008.
17. Martínez-Abad, A.; González-Ausejo, J.; Lagarón, J. M.; Cabedo, L. *Polym. Degrad. Stab.* **2016**, *132*, 52.
18. Misra, M.; Pandey, J. K.; Mohanty, A. K. Biocomposites: Design and Mechanical Performance; Elsevier Inc., **2015**.
19. Sanchez-Safont, E. L.; Gonzalez-Ausejo, J.; Gamez-Perez, J.; Lagaron, J. M.; Cabedo, L. *J. Renew. Mater.* **2016**, *4*.
20. Carli, L. N.; Crespo, J. S.; Mauler, R. S. *Compos. Part A: Appl. Sci. Manuf.* **2011**, *42*, 1601.
21. Barham, P. J.; Keller, A.; Otun, E. L.; Holmes, P. A. *J. Mater. Sci.* **1984**, *19*, 2781.
22. Cheng, M.-L.; Sun, Y.-M. *Polymer.* **2009**, *50*, 5298.
23. UNE-EN ISO UNE-EN ISO 20200 Determinación del grado de desintegración de materiales plásticos bajo condiciones de compostaje simuladas en un laboratorio **2006**.
24. Hameed, N.; Guo, Q.; Tay, F. H.; Kazarian, S. G. *Carbohydr. Polym.* **2011**, *86*, 94.

25. Wang, S.; Xiang, H.; Wang, R.; Peng, C.; Zhou, Z.; Zhu, M. *Polym. Eng. Sci.* **2014**, *54*, 1113.
26. Nagarajan, V.; Misra, M.; Mohanty, A. K. *Ind. Crops Prod.* **2013**, *42*, 461.
27. Berthet, M.-A.; Mayer-Laigle, C.; Rouau, X.; Gontard, N.; Angellier-Coussy, H. *Compos. Part A: Appl. Sci. Manuf.* **2017**, *95*, 12.
28. Berthet, M.; Angellier-coussy, H.; Machado, D.; Hilliou, L.; Staebler, A.; Vicente, A.; Gontard, N. *Ind. Crops Prod.* **2015**, *69*, 110.
29. Gatenholm, P.; Kubát, J.; Mathiasson, A. *J. Appl. Polym. Sci.* **1992**, *45*, 1667.
30. Liu, Q.-S.; Zhu, M.-F.; Wu, W.-H.; Qin, Z.-Y. *Polym. Degrad. Stab.* **2009**, *94*, 18.
31. Sanchez-Garcia, M. D.; Lagaron, J. M. *Cellulose.* **2010**, *17*, 987.
32. Barick, A. K.; Tripathy, D. K. *Mater. Sci. Eng. A.* **2010**, *527*, 812.
33. Herrera, M.; Matuschek, G.; Kettrup, A. *Polym. Degrad. Stab.* **2002**, *78*, 323.
34. Srithep, Y.; Ellingham, T.; Peng, J.; Sabo, R.; Clemons, C.; Turng, L.-S.; Pilla, S. *Polym. Degrad. Stab.* **2013**, *98*, 1439.
35. Bhardwaj, R.; Mohanty, A. K.; Drzal, L. T.; Pourboghrat, F.; Misra, M. *Biomacromolecules.* **2006**, *7*, 2044.
36. Rossa, L. V.; Scienza, L. C.; Zattera, A. *J. Polym. Compos.* **2013**, *34*, 450.
37. Nagarajan, V.; Mohanty, A. K.; Misra, M. *ACS Sustain. Chem. Eng.* **2016**, *4*, 2899.
38. Kim, Y. D.; Kim, S. C. *Polym. Degrad. Stab.* **1998**, *62*, 343.
39. Howard, G. T. *Int. Biodeterior. Biodegradation.* **2002**, *49*, 245.
40. Weng, Y.-X.; Wang, Y.; Wang, X.-L.; Wang, Y.-Z. *Polym. Test.* **2010**, *29*, 579.
41. Arrieta, M. P.; López, J.; Rayón, E.; Jiménez, A. *Polym. Degrad. Stab.* **2014**, *1*. Q17
42. Puglia, D.; Fortunati, E.; D'Amico, D. a.; Manfredi, L. B.; Cyras, V. P.; Kenny, J. M. *Polym. Degrad. Stab.* **2014**, *99*, 127.
43. González-Ausejo, J.; Sanchez-Safont, E.; Lagaron, J. M.; Olsson, R. T.; Gamez-Perez, J.; Cabedo, L. *Polym. Test.* **2017**, *62*, 235.
44. Sánchez-Safont, E. L.; Aldureid, A.; Lagarón, J. M.; Gámez-Pérez, J.; Cabedo, L. *Compos. Part B: Eng.* **2018**, *145*, 215.
45. Utracki, L. A.; Kamal, M. R. *Polym. Eng. Sci.* **1982**, *22*, 96.
46. Carley, J. F.; Crossan, S. C. **1980**, 285.

Graphical abstract

PHBV/TPU/cellulose compounds for compostable injection molded parts with improved thermal and mechanical performance

Estefanía Lidón Sánchez-Safont, Alex Arrillaga, Jon Anakabe, José Gamez-Perez and Luis Cabedo

Q6